frontiers | Frontiers in Physics

TYPE Original Research
PUBLISHED 25 November 2022
DOI 10.3389/fphy.2022.1071200



OPEN ACCESS

EDITED BY
Fei Yu,
Changsha University of Science and Technology, China

REVIEWED BY
Ji-Huan He,
Soochow University, China
Kangsheng Zhao,
Fudan University, China
Rongfei Xu,
Nanjing Normal University, China

*CORRESPONDENCE
Baojian Hong,
hbj@njit.edu.cn

SPECIALTY SECTION
This article was submitted to Interdisciplinary Physics, a section of the journal Frontiers in Physics

RECEIVED 15 October 2022
ACCEPTED 26 October 2022
PUBLISHED 25 November 2022

CITATION
Hong B (2022), Assorted exact explicit solutions for the generalized Atangana's fractional BBM–Burgers equation with the dissipative term.
*Front. Phys.* 10:1071200.
doi: 10.3389/fphy.2022.1071200



# Assorted exact explicit solutions for the generalized Atangana's fractional BBM–Burgers equation with the dissipative term

Baojian Hong*

Faculty of Mathematical Physics, Nanjing Institute of Technology, Nanjing, China

In this study, the generalized Atangana's fractional BBM–Burgers equation (GBBM-B) with the dissipative term is investigated by utilizing the modified sub-equation method and the new *G′/(bG′ + G + a)*-expansion method; with the aid of symbolic computations, many types of new exact explicit solutions including solitary wave solutions, trigonometric function periodic solutions, and the rational function solutions are obtained. Some 3D and 2D plots of these solutions are simulated, which show the novelty and visibility of the propagation behavior and dynamical structure of the corresponding equation. Moreover, with the selection of different values on the parameters and orders, we can deduce many types of exact solutions in special cases. We also discussed the changes and characteristics of these solutions, which can help us further understand the inner structure of this equation. The obtained solutions indicate that the approach is easy and effective for nonlinear models with high-order dispersion terms.

KEYWORDS

**generalized BBM–Burgers equation, Atangana's fractional derivative, dissipative term, modified sub-equation method, *G′/(bG′ + G + a)*-expansion method, exact solutions**

## 1 Introduction

As is known, calculus was founded by Newton and Leibniz at the end of the 1660s, and fractional order calculus has gradually become one of the new special fields in natural sciences and mathematical physics since 1695 [1]. In recent years, due to the wide application of fractional order calculus in nonlinear partial differential equations (PDEs), especially fractional PDEs [2–4], many nonlinear phenomena come down to fractional models, such as ecological and economic systems [5], two-scale thermal science [6], mechanics [7], chaotic oscillations [8], atmospheric science [9], and optical fiber [10–12]. Searching for exact explicit solutions of these nonlinear fractional PDEs plays a significant role in the study of the dynamics of those phenomena. Until now, many powerful methods for this subject have been offered, such as the Darboux transformation [13], Bäcklund transformation method [14], and Hirota bilinear method [15], which can be

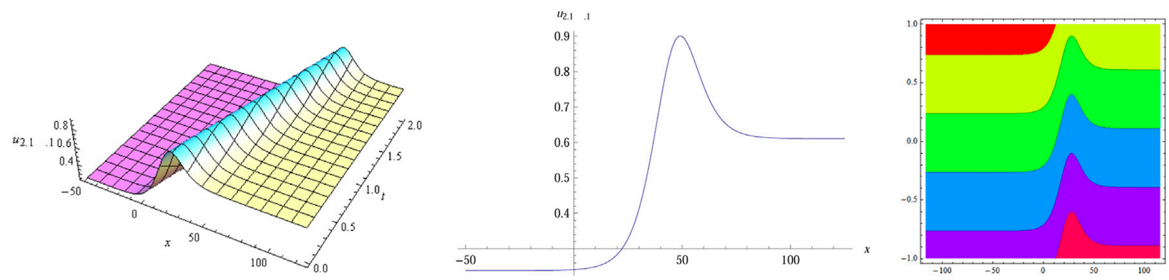

**FIGURE 1**
3D plot, 2D plot, and contour plot of $u_{2.1.1}$ with $\alpha = 1, \beta = 1$.

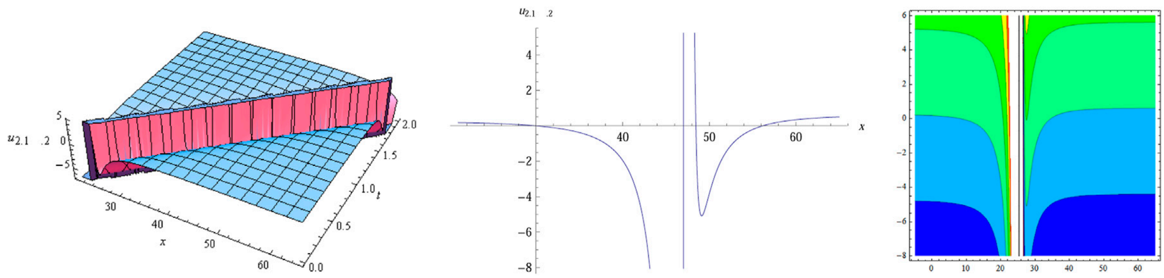

**FIGURE 2**
3D plot, 2D plot, and contour plot of $u_{2.1.2}$ with $\alpha = 1, \beta = 1$.

used to find N-soliton solutions. The improved F-expansion method [16], projective Riccati equation method [17], sine-Gordon method [18], Jacobi elliptic function expansion method [19], G'/G-expansion method [20], (G'/G,1/G)-expansion method [21], improved (m + G'/G)-expansion method [22], improved G'/G$^2$-expansion method [23], exp (−φ(ξ)) technique [24], homogeneous balance method [25], first integral method [26], inverse scattering transformation [27], and Lie symmetry method [28], etc [29–34] can be used to find Jacobi periodic solutions, solitary wave solutions, and trigonometric function solutions of these models. Until now, there are many types of definitions for the fractional derivative, and the most classic definitions are as follows:

Riemann–Liouville fractional derivative [35]:

$$D_t^\alpha f(t)=\begin{cases}\dfrac{1}{\Gamma(n-\alpha)}\dfrac{d^n}{dt^n}\displaystyle\int_0^t (t-\tau)^{n-\alpha-1} f(\tau)d\tau, n-1<\alpha<n, n\in N.\\ \dfrac{d^{(n)}f(t)}{dt^n}, \alpha=n\in N.\end{cases}$$

Caputo fractional derivative [36]:

$$D_t^\alpha f(t)=\begin{cases}\dfrac{1}{\Gamma(n-\alpha)}\displaystyle\int_0^t (t-\tau)^{n-\alpha-1} f^{(n)}(\tau)d\tau, n-1<\alpha<n, n\in N.\\ \dfrac{d^{(n)}f(t)}{dt^n}, \alpha=n\in N.\end{cases}$$

Jumarie's fractional derivative [37]:

$$D_t^\alpha f(t)=\begin{cases}\dfrac{1}{\Gamma(1-\alpha)}\dfrac{d}{dt}\displaystyle\int_0^t (t-\tau)^{-\alpha}\left[f(\tau)-f(0)\right]d\tau, 0<\alpha<1,\\ \left(f^{(n)}(t)\right)^{(\alpha-n)}, n\le\alpha<n+1, n\in N^+.\end{cases}$$

Ji-Huan He's fractional derivative [38]:

$$D_t^\alpha f(t)=\begin{cases}\dfrac{1}{\Gamma(n-\alpha)}\dfrac{d^n}{dt^n}\displaystyle\int_{t_0}^t (\tau-t)^{n-\alpha-1}\left[f_0(\tau)-f(\tau)\right]\\ d\tau, n-1<\alpha<n, n\in N.\\ \dfrac{d^{(n)}f(t)}{dt^n}, \alpha=n\in N.\end{cases}$$

Furthermore, the Atangana–Baleanu derivative [39], M-fractional derivative [40], conformable fractional derivative [41], and Atangana's fractional derivative [42, 43] which will be utilized in this article, are built recently.

In this paper, we consider the generalized Atangana's fractional BBM–Burgers equation with the dissipative term in the following form [44–47]:

$$D_t^\alpha u + \rho D_x^\beta u + \sigma u D_x^\beta u - \mu D_x^{2\beta} u - \delta D_t^\alpha D_x^{2\beta} u + \gamma D_x^{4\beta} u = 0, \quad 0<\alpha,\beta\le 1, \tag{1}$$

where $D_t^\alpha(\cdot), D_x^\beta(\cdot)$ are the Atangana's fractional derivative [42] $(\cdot)_t^\alpha = {}_0^A D_t^\alpha(\cdot)$, $(\cdot)_x^\beta = {}_0^A D_x^\beta(\cdot)$, $(\cdot)_x^{2\beta} = {}_0^A D_x^\beta({}_0^A D_x^\beta(\cdot))$, $(\cdot)_x^{4\beta} = {}_0^A D_x^\beta({}_0^A D_x^\beta({}_0^A D_x^\beta({}_0^A D_x^\beta(\cdot))))$.

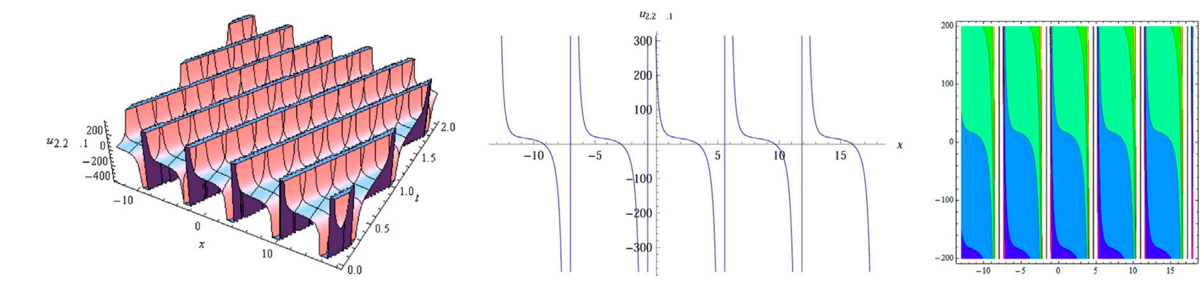


FIGURE 3
3D plot, 2D plot, and contour plot of $u_{2.2.1}$ with $\alpha = 1, \beta = 1$.

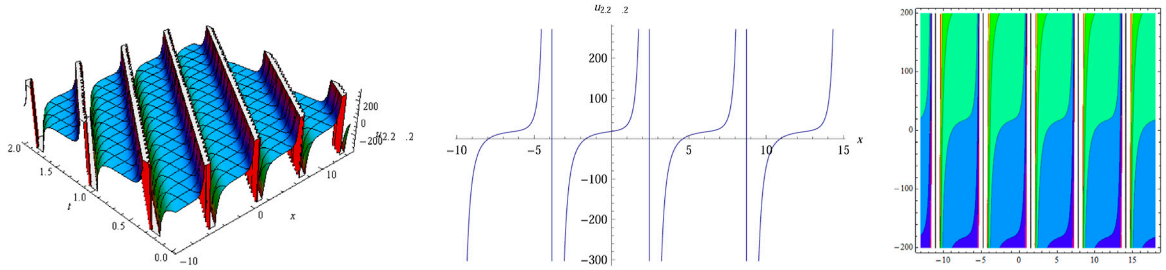


FIGURE 4
3D plot, 2D plot, and contour plot of $u_{2.2.2}$ with $\alpha = 1, \beta = 1$.

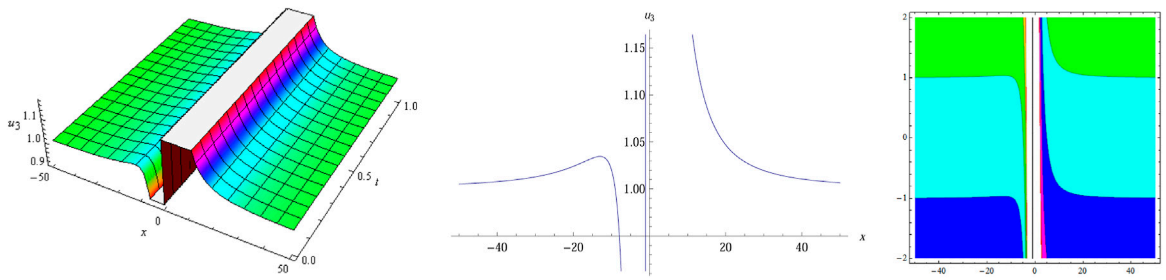


FIGURE 5
3D plot, 2D plot, and contour plot of $u_3$ with $\alpha = \beta = 1$.

The coefficients $\rho, \sigma, \mu, \delta, \gamma$ are real constants; when $\mu = \gamma = 0, \alpha = \beta = 1$, or $\beta = 1, 0 < \alpha \le 1$, Eq. 1 is related to the well-known BBM equation or fractional BBM equation, which was proposed by Benjamin–Bona–Mahony and describes approximately the unidirectional propagation of a long wave in certain nonlinear dispersive systems as a refinement of the KdV equation [48–51]. When $\delta = \gamma = 0, \alpha = 1$ or $\beta = 1, 0 < \alpha \le 1$, Eq. 1 is related to the well-known Burgers equation [52, 53]. Some related research studies about Eq. 1 can be found in [45, 54, 55].

Next, we review some basic definitions and properties of the Atangana fractional derivative which are used further in this paper [42, 43].

**Definition:** For a function $f(t)$: $[0, \infty) \to R$, we defined the Atangana fractional derivative operator and integral operator of $f(t)$ of the order $\alpha$ as [42, 43]

$$D_t^\alpha f(t) = {}_0^A D_t^\alpha f(t) = \lim_{\varepsilon \to 0} \frac{f\left(t + \varepsilon \left(t + \frac{1}{\Gamma(\alpha)}\right)^{1-\alpha}\right) - f(t)}{\varepsilon}, \quad 0 < \alpha \le 1,$$

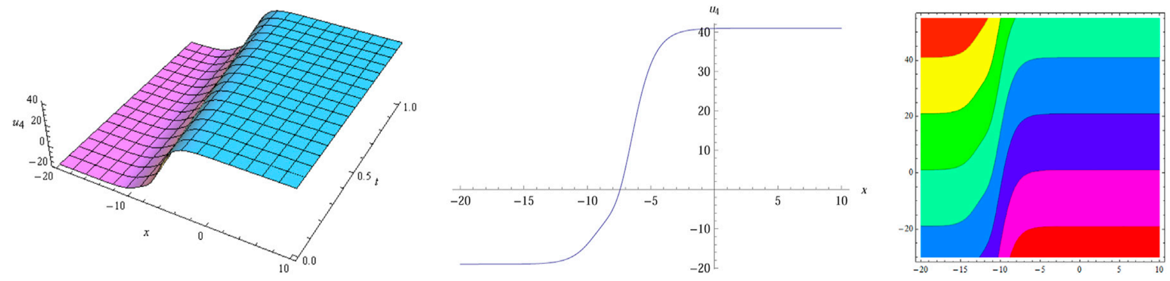


FIGURE 6
3D plot, 2D plot, and contour plot of $u_4$ with $\alpha = \beta = 1$.

$$I_t^{\alpha} f(t) = {}_0^A I_t^{\alpha} f(t) = \int_0^t f(\tau)\left(\tau + \frac{1}{\Gamma(\alpha)}\right)^{\alpha-1} d\tau, \quad 0 < \alpha \leq 1.$$

Also, we have the following important properties [42, 43]:

(1) ${}_0^A D_t^{\alpha} f(t) = \left(t + \frac{1}{\Gamma(\alpha)}\right)^{1-\alpha} \frac{df(t)}{dt}.$

(2) ${}_0^A D_t^{\alpha}(af(t) + bg(t)) = a_0^A D_t^{\alpha} f(t) + b_0^A D_t^{\alpha} g(t), \forall a, b \in R.$

(3) ${}_0^A D_t^{\alpha}(f(t)g(t)) = f(t)_0^A D_t^{\alpha} g(t) + g(t)_0^A D_t^{\alpha} f(t).$

(4) ${}_0^A D_t^{\alpha}(f(t)/g(t)) = \left[g(t)_0^A D_t^{\alpha} f(t) - f(t)_0^A D_t^{\alpha} g(t)\right]/g^2(t).$

(5) ${}_0^A D_t^{\alpha}(f \circ g)(t) = f'(g(t))_0^A D_t^{\alpha} g(t) = \left(t + \frac{1}{\Gamma(\alpha)}\right)^{1-\alpha} f'(g(t)) \frac{dg(t)}{dt}.$

The rest of the paper is organized as follows. In Section 2, we introduce the modified sub-equation method [56–59] and the new G'/(bG'+G+a)-expansion method, while in Section 3, some exact solutions of the GBBM–Burgers equation are found and discussed by utilizing the proposed methods. Finally, the conclusion is presented in Section 4.

## 2 Description of the two methods

### 2.1 The modified sub-equation method

Consider the following Atangana's fractional differential equation:

$$P\left(u, u_t^{\alpha}, u_x^{\beta}, u_x^{2\beta}, u_x^{3\beta}, u_x^{4\beta}, uu_x^{\beta}, \cdots\right) = 0. \tag{2}$$

We use the following wave transformation [60]:

$$u(x,t) = u(\xi), \xi = \frac{k}{\beta}\left(x + \frac{1}{\Gamma(\beta)}\right)^{\beta} + \frac{w}{\alpha}\left(t + \frac{1}{\Gamma(\alpha)}\right)^{\alpha} \tag{3}$$

where the constant $k$ means the wave number which can reflect the frequency and w is the wave speed. Thus, Eq. 2 reduces to an ordinary differential equation:

$$O\left(u, u', u'', u''', u^{(4)}, uu', \cdots\right) = 0. \tag{4}$$

Assume that Eq. 4 has the following solution:

$$u = \sum_{i=0}^{N} A_i F^i, \tag{5}$$

where $N$ is a balance number, $F = F(\xi)$, and $A_i$ and the variable function $\xi = \xi(x,t)$ are determined later. The function $F$ satisfies the Riccati equation defined by

$$F' = \frac{dF(\xi)}{d\xi} = b + dF^2(\xi) = b + dF^2, b, d \in R. \tag{6}$$

Equation 6 gives the following solutions:

$$F = \begin{cases} F_1 = \begin{cases} F_{1.1} = -\sqrt{-\Delta}\tanh\left(d\sqrt{-\Delta}\,\xi\right), \\ F_{1.2} = -\sqrt{-\Delta}\coth\left(d\sqrt{-\Delta}\,\xi\right), \\ F_{1.3} = -\sqrt{-\Delta}\tanh\left(2d\sqrt{-\Delta}\,\xi\right) \pm i\sqrt{-\Delta}\operatorname{sec}h\left(2d\sqrt{-\Delta}\,\xi\right), \end{cases}, \Delta = \frac{b}{d} < 0, \\ F_2 = \begin{cases} F_{2.1} = \sqrt{\Delta}\tan\left(d\sqrt{\Delta}\,\xi\right), \\ F_{2.2} = -\sqrt{\Delta}\cot\left(d\sqrt{\Delta}\,\xi\right), \\ F_{2.3} = \sqrt{\Delta}\tan\left(2d\sqrt{\Delta}\,\xi\right) \pm \sqrt{\Delta}\sec\left(2d\sqrt{\Delta}\,\xi\right). \end{cases}, \Delta = \frac{b}{d} > 0, \\ F_3 = -\frac{d}{\xi + \xi_0}, \Delta = \frac{b}{d} = 0, \xi_0 \in R. \end{cases}$$

When $d = 1$, we can obtain the results mentioned in [56–59].

Substituting Eqs 6, 5 into Eq. 4, collecting the coefficients of $F^i\,(i = 0, 1, 2, \cdots)$ to zero yields algebraic equations (AEs) for $A_0, A_1, \cdots, A_N$ and $\xi$. Utilizing mathematical software to solve the AEs, we can obtain the solutions of Eq. 4.

### 2.2 The $G'/(bG' + G + a)$-expansion method

With similar steps to technique Section 2.1, we give the main steps of this method.

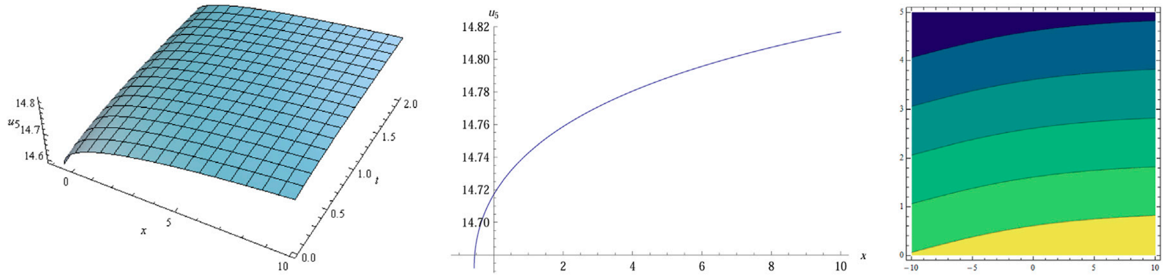


FIGURE 7
3D plot, 2D plot, and contour plot of $u_5$ with $\alpha = 0.3, \beta = 0.5$.

**Step 1:** Assume that Eq. 4 has the following solution:

$$u = \sum_{i=0}^{N} a_i F^i, \tag{7}$$

where $F = F(\xi) = \frac{G'}{bG'+G+a}$, and $a_i$ and the variable function $\xi = \xi(x,t)$ are determined later. The parameters $a$ and $b \neq 0$ are arbitrary constants, and $G = G(\xi)$ is a solution of the following auxiliary ODE:

$$G'' = -\frac{\lambda}{b}G' - \frac{\mu}{b^2}G - \frac{\mu}{b^2}a, \tag{8}$$

where $\lambda, \mu$ are two arbitrary real numbers. We can find the following constrained condition:

$$F' = (\lambda - \mu - 1)F^2 + \frac{1}{b}(2\mu - \lambda)F - \frac{1}{b^2}\mu. \tag{9}$$

Equation 9 gives the following solutions:

**Case 1:** When $\Delta = \lambda^2 - 4\mu > 0$, we have $G = -a + p_1 e^{\frac{1}{2b}(-\lambda-\sqrt{\Delta})\xi} + p_2 e^{\frac{1}{2b}(-\lambda+\sqrt{\Delta})\xi}$, and $a, p_1, p_2$ are arbitrary constants that satisfy $a^2 + p_1^2 + p_2^2 \neq 0$, as in case 2; thus,

$$F_1 = \frac{p_1(\lambda+\sqrt{\Delta}) + p_2(\lambda-\sqrt{\Delta})e^{\frac{\sqrt{\Delta}}{b}\xi}}{bp_1(\lambda-2+\sqrt{\Delta}) + bp_2(\lambda-2-\sqrt{\Delta})e^{\frac{\sqrt{\Delta}}{b}\xi}}$$

$$= \frac{[\lambda(p_2-p_1) - \sqrt{\Delta}(p_2+p_1)]\sinh(\frac{\sqrt{\Delta}}{2b}\xi) + [\lambda(p_2+p_1) - \sqrt{\Delta}(p_2-p_1)]\cosh(\frac{\sqrt{\Delta}}{2b}\xi)}{b[(\lambda-2)(p_2-p_1) - \sqrt{\Delta}(p_2+p_1)]\sinh(\frac{\sqrt{\Delta}}{2b}\xi) + b[(\lambda-2)(p_2+p_1) - \sqrt{\Delta}(p_2-p_1)]\cosh(\frac{\sqrt{\Delta}}{2b}\xi)},$$

$$F_1 = \begin{cases} F_{1.1} = \frac{\lambda-2\mu}{2b(\lambda-\mu-1)} - \frac{\sqrt{\Delta}}{2b(\lambda-\mu-1)}\tanh\left(\frac{\sqrt{\Delta}}{2b}\xi\right), (\lambda-2)(p_2-p_1) - \sqrt{\Delta}(p_2+p_1) = 0, \\ F_{1.2} = \frac{\lambda-2\mu}{2b(\lambda-\mu-1)} - \frac{\sqrt{\Delta}}{2b(\lambda-\mu-1)}\coth\left(\frac{\sqrt{\Delta}}{2b}\xi\right), (\lambda-2)(p_2+p_1) - \sqrt{\Delta}(p_2-p_1) = 0. \end{cases}$$

**Case 2:** When $\Delta = \lambda^2 - 4\mu < 0$, we have $G = e^{-\frac{\lambda}{2b}\xi}\left(p_1\cos(\frac{\sqrt{-\Delta}}{2b}\xi) + p_2\sin(\frac{\sqrt{-\Delta}}{2b}\xi)\right) - a$,

$$F_2 = \frac{(\lambda p_1 - \sqrt{-\Delta}\,p_2)\cos\left(\frac{\sqrt{-\Delta}}{2b}\xi\right) + (\lambda p_2 + \sqrt{-\Delta}\,p_1)\sin\left(\frac{\sqrt{-\Delta}}{2b}\xi\right)}{b((\lambda-2)p_1 - \sqrt{-\Delta}\,p_2)\cos\left(\frac{\sqrt{-\Delta}}{2b}\xi\right) + b((\lambda-2)p_2 + \sqrt{-\Delta}\,p_1)\sin\left(\frac{\sqrt{-\Delta}}{2b}\xi\right)}$$

$$F_2 = \begin{cases} F_{2.1} = \frac{\lambda-2\mu}{2b(\lambda-\mu-1)} + \frac{\sqrt{-\Delta}}{2b(\lambda-\mu-1)}\tan\left(\frac{\sqrt{-\Delta}}{2b}\xi\right), (\lambda-2)p_2 + \sqrt{-\Delta}p_1 = 0, \\ F_{2.2} = \frac{\lambda-2\mu}{2b(\lambda-\mu-1)} - \frac{\sqrt{-\Delta}}{2b(\lambda-\mu-1)}\cot\left(\frac{\sqrt{-\Delta}}{2b}\xi\right), (\lambda-2)p_1 - \sqrt{-\Delta}p_2 = 0. \end{cases}$$

**Step 2:** Substituting Eqs 7, 9 into Eq. 4 and setting the coefficients of $F^i$ zero yield a set of AEs for $a_i, b, \lambda, \mu, k$ and $w$. After solving the AEs and substituting each of the solutions $F_1, F_2$ along with Eqs 7, 3 into Eq. 2, we can obtain the solutions of Eq. 2.

In the following section, we will use these two methods to solve the GBBM–Burgers equation.

# 3 Exact solutions to the GBBM–Burgers equation

## 3.1 Using the modified sub-equation method

Substituting Eq. 3 into Eq. 1 and integrating Eq. 1 once, we have

$$(w + k\rho)u + \frac{k\sigma}{2}u^2 - \mu k^2 u' - \delta w k^2 u'' + \gamma k^4 u''' = A, \tag{10}$$

where $A$ is the integral constant. By balancing the highest derivative term with the nonlinear terms in Eq. 10, we obtain $N = 3$. Therefore, we assume that Eq. 10 has the following solutions:

$$u = A_0 + A_1 F + A_2 F^2 + A_3 F^3, \tag{11}$$

where $A_0, A_1, A_2, A_3$ are constants to be determined later. Substituting Eqs 11, 6 into Eq. 10, collecting the coefficients of $F^i\,(i = 0, 1, 2, \cdots)$ to zero, we have

$$\begin{aligned} F^0 &: 2\left(A + bk^2\left(-2bdk^2\gamma + \mu\right)A_1 + 2b^2k^2w\delta A_2 - 6b^3k^4\gamma A_3\right) \\ &\quad = A_0\left(2(w + k\rho) + k\sigma A_0\right), \\ F^1 &: \left(w - 2bdk^2w\delta + k\rho + k\sigma A_0\right)A_1 + 2bk^2\left(\left(8bdk^2\gamma - \mu\right)A_2 \right. \\ &\qquad \left. - 3bw\delta A_3\right) = 0, \\ F^2 &: dk^2\left(8bdk^2\gamma - \mu\right)A_1 + \frac{1}{2}k\sigma A_1^2 + \left(w - 8bdk^2w\delta + k\rho + k\sigma A_0\right)A_2 \\ &\quad + 3bk^2\left(20bdk^2\gamma - \mu\right)A_3 = 0, \\ F^3 &: 2dk^2\left(20bdk^2\gamma - \mu\right)A_2 + kA_1\left(-2d^2kw\delta + \sigma A_2\right) \\ &\quad + \left(w - 18bdk^2w\delta + k\rho + k\sigma A_0\right)A_3 = 0, \end{aligned}$$

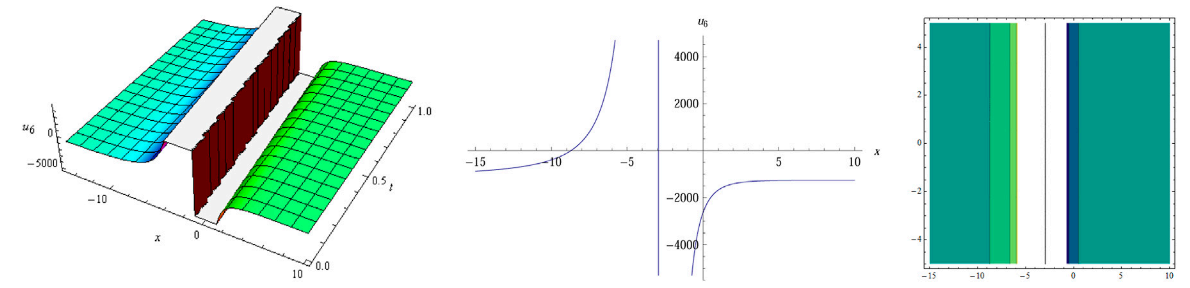


FIGURE 8
3D plot, 2D plot, and contour plot of $u_6$ with $\alpha = \beta = 1$.

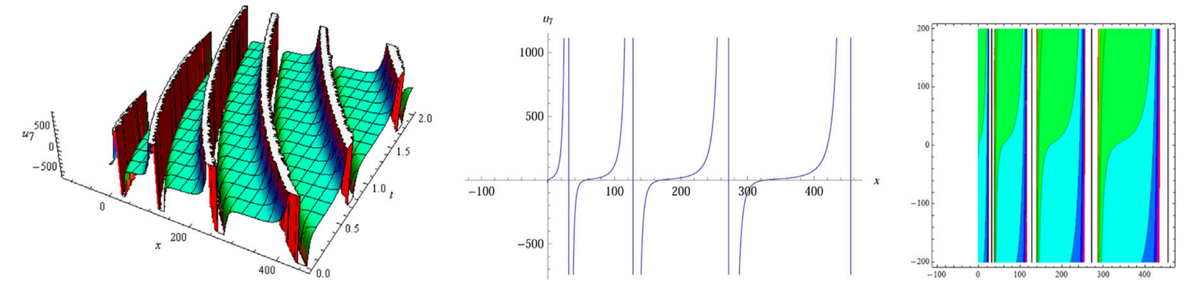


FIGURE 9
3D plot, 2D plot, and contour plot of $u_7$ with $\alpha = 0.6, \beta = 0.6$.

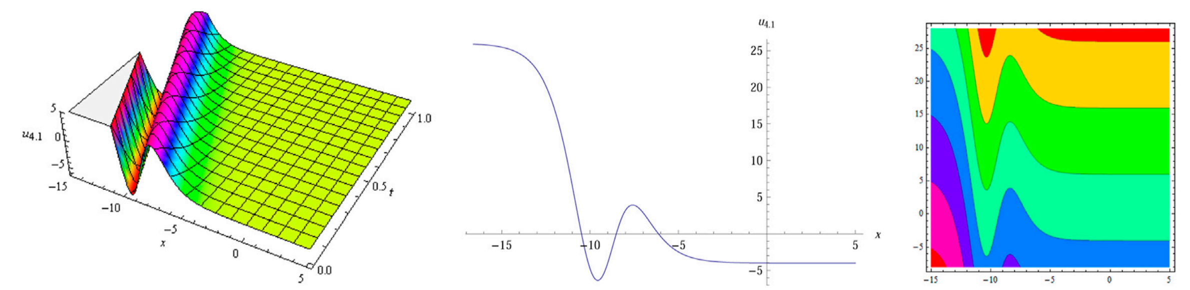


FIGURE 10
3D plot, 2D plot, and contour plot of $u_{4.1}$ with $\alpha = \beta = 1$.

$$F^4:\ k\left(-12d^2kw\delta A_2 + \sigma A_2^2 + 6dk\left(38bdk^2\gamma - \mu\right)A_3 + 2A_1\left(6d^3k^3\gamma + \sigma A_3\right)\right) = 0,$$

$$F^5:\ k\left(-12d^2kw\delta A_3 + A_2\left(24d^3k^3\gamma + \sigma A_3\right)\right) = 0,$$

$$F^6:\ kA_3\left(120d^3k^3\gamma + \sigma A_3\right) = 0.$$

Solving the aforementioned AEs, we have the following cases:

**Case 1:**

$$A_0 = \pm\frac{4\gamma\sqrt{-\mu} + \left(11\delta\mu\sqrt{-\mu} \mp \sqrt{\gamma}\,\delta\rho\right)}{\sqrt{\gamma}\,\delta\sigma}, A_1 = \frac{30dk\mu}{\sigma},$$
$$A_2 = \frac{15d^2kw\delta}{\sigma}, A_3 = -\frac{120d^3k^3\gamma}{\sigma},$$
$$A = \frac{k\left(16\mu\left(\gamma^2 - \delta^2\mu^2\right) - \gamma\delta^2\rho^2\right)}{2\gamma\delta^2\sigma} - \frac{4k\sqrt{-\gamma\mu}\rho}{\delta\sigma}, w = \mp\frac{4k\sqrt{-\gamma\mu}}{\delta}, b = -\frac{\mu}{4dk^2\gamma}.$$

**Case 2:**

$$A_0=\pm\frac{564\gamma\sqrt{-47\mu}-45\delta\mu\sqrt{-47\mu}\mp 2209\delta\rho\sqrt{\gamma}}{2209\sqrt{\gamma}\delta\sigma},A_1=\frac{90dk\mu}{47\sigma},$$
$$A_2=\frac{15d^2kw\delta}{\sigma},A_3=-\frac{120d^3k^3\gamma}{\sigma},$$
$$A=-\frac{k\rho^2}{2\sigma}+\frac{144k\mu\left(2209\gamma^2-25\delta^2\mu^2\right)\pm 53016\sqrt{47}k\gamma\delta\sqrt{-\gamma\mu}\rho}{207646\gamma\delta^2\sigma},$$
$$w=\mp\frac{12k\sqrt{-\gamma\mu}}{\sqrt{47}\delta},b=\frac{\mu}{188dk^2\gamma}.$$

We can obtain the following traveling wave solutions.

**Family 1** $\Delta=\frac{b}{d}<0,d\neq 0$

**Set 1**

$$u_{1.1}=\pm\frac{4\gamma\sqrt{-\mu}+\left(11\delta\mu\sqrt{-\mu}\mp\sqrt{\gamma}\delta\rho\right)}{\sqrt{\gamma}\delta\sigma}+\frac{30dk\mu}{\sigma}F_1(\xi_{1.1})+\frac{15d^2kw\delta}{\sigma}F_1^2(\xi_{1.1})-\frac{120d^3k^3\gamma}{\sigma}F_1^3(\xi_{1.1}),$$

$$u_{2.1}=\pm\frac{(564\gamma-45\delta\mu)\sqrt{-47\mu}\mp 2209\delta\rho\sqrt{\gamma}}{2209\sqrt{\gamma}\delta\sigma}+\frac{90dk\mu}{47\sigma}F_2(\xi_{2.1})+\frac{15d^2kw\delta}{\sigma}F_2^2(\xi_{2.1})-\frac{120d^3k^3\gamma}{\sigma}F_2^3(\xi_{2.1}),$$

where $F_1(\xi_{1.1})=\begin{cases}F_{1.1.1}=-\sqrt{\frac{\mu}{4d^2k^2\gamma}}\tanh\xi_{1.1},F_{1.1.2}=-\sqrt{\frac{\mu}{4d^2k^2\gamma}}\coth\xi_{1.1},\\ F_{1.1.3}=-\sqrt{\frac{\mu}{4d^2k^2\gamma}}[\tanh(2\xi_{1.1})\pm i\,sech(2\xi_{1.1})].\end{cases}$

$$\xi_{1.1}=\sqrt{\frac{\mu}{4\gamma}}\left[\frac{1}{\beta}\left(x+\frac{1}{\Gamma(\beta)}\right)^{\beta}\mp\frac{4\sqrt{-\gamma\mu}}{\alpha\delta}\left(t+\frac{1}{\Gamma(\alpha)}\right)^{\alpha}\right],$$
$$w=\mp\frac{4k\sqrt{-\gamma\mu}}{\delta}.$$

$$F_2(\xi_{2.1})=\begin{cases}F_{2.1.1}=-\sqrt{-\frac{\mu}{188d^2k^2\gamma}}\tanh\xi_{2.1},F_{2.1.2}=-\sqrt{-\frac{\mu}{188d^2k^2\gamma}}\coth\xi_{2.1},\\ F_{2.1.3}=-\sqrt{-\frac{\mu}{188d^2k^2\gamma}}[\tanh(2\xi_{2.1})\pm i\,sech(2\xi_{2.1})].\end{cases}$$

$$\xi_{2.1}=\sqrt{-\frac{\mu}{188\gamma}}\;\frac{1}{\beta}\left(x+\frac{1}{\Gamma(\beta)}\right)^{\beta}\mp\frac{12\sqrt{-\gamma\mu}}{\sqrt{47}\delta\alpha}\left(t+\frac{1}{\Gamma(\alpha)}\right)^{\alpha},$$
$$w=\mp\frac{12k\sqrt{-\gamma\mu}}{\sqrt{47}\delta}.$$

The numerical simulation of $u_{2.1.1},u_{2.1.2}$ is shown in Figures 1, 2, where we select

$$d=1,k=1,\mu=-1,\gamma=1,\delta=1,\rho=1,\sigma=1,w=-12/\sqrt{47},$$
$$A_0=-1+609\sqrt{47}/2209,A_1=-90/47,A_2=600/\sqrt{47},$$
$$A_3=-120,w=-12/\sqrt{47},\alpha=\beta=1.$$

**Family 2** $\Delta=\frac{b}{d}>0,d\neq 0$

**Set 2**

$$u_{1.2}=\pm\frac{4\gamma\sqrt{-\mu}+\left(11\delta\mu\sqrt{-\mu}\mp\sqrt{\gamma}\delta\rho\right)}{\sqrt{\gamma}\delta\sigma}+\frac{30dk\mu}{\sigma}F_1(\xi_{1.2})+\frac{15d^2kw\delta}{\sigma}F_1^2(\xi_{1.2})-\frac{120d^3k^3\gamma}{\sigma}F_1^3(\xi_{1.2}),$$

$$u_{2.2}=\pm\frac{(564\gamma-45\delta\mu)\sqrt{-47\mu}\mp 2209\delta\rho\sqrt{\gamma}}{2209\sqrt{\gamma}\delta\sigma}+\frac{90dk\mu}{47\sigma}F_2(\xi_{2.2})+\frac{15d^2kw\delta}{\sigma}F_2^2(\xi_{2.2})-\frac{120d^3k^3\gamma}{\sigma}F_2^3(\xi_{2.2}),$$

where

$$F_1(\xi_{1.2})=\begin{cases}F_{1.2.1}=\sqrt{-\frac{\mu}{4d^2k^2\gamma}}\tan\xi_{1.2},F_{1.2.2}=-\sqrt{-\frac{\mu}{4d^2k^2\gamma}}\cot\xi_{1.2},\\ F_{1.2.3}=\sqrt{-\frac{\mu}{4d^2k^2\gamma}}[\tan(2\xi_{1.2})\pm sec(2\xi_{1.2})].\end{cases}$$

$$\xi_{1.2}=\sqrt{-\frac{\mu}{4\gamma}}\left[\frac{1}{\beta}\left(x+\frac{1}{\Gamma(\beta)}\right)^{\beta}\mp\frac{4\sqrt{-\gamma\mu}}{\alpha\delta}\left(t+\frac{1}{\Gamma(\alpha)}\right)^{\alpha}\right],$$
$$w=\mp\frac{4k\sqrt{-\gamma\mu}}{\delta}.$$

$$F_2(\xi_{2.2})=\begin{cases}F_{2.2.1}=\sqrt{\frac{\mu}{188d^2k^2\gamma}}\tan\xi_{2.2},F_{2.2.2}=-\sqrt{\frac{\mu}{188d^2k^2\gamma}}\cot\xi_{2.2},\\ F_{2.2.3}=\sqrt{\frac{\mu}{188d^2k^2\gamma}}[\tan(2\xi_{2.2})\pm sec(2\xi_{2.2})].\end{cases}$$

$$\xi_{2.2}=\sqrt{\frac{\mu}{188k^2\gamma}}\left[\frac{1}{\beta}\left(x+\frac{1}{\Gamma(\beta)}\right)^{\beta}\mp\frac{12\sqrt{-\gamma\mu}}{\sqrt{47}\delta\alpha}\left(t+\frac{1}{\Gamma(\alpha)}\right)^{\alpha}\right],$$
$$w=\mp\frac{12k\sqrt{-\gamma\mu}}{\sqrt{47}\delta}.$$

The numerical simulation of $u_{2.2.1},u_{2.2.2}$ is shown in Figures 3, 4, where we select

$$d=1,k=1,\mu=-1,\gamma=1,\delta=1,\rho=1,\sigma=1,w=-4,$$
$$A_0=14,A_1=-30,A_2=-60,A_3=-120,\alpha=\beta=1.$$

**Family 3** $\Delta=\frac{b}{d}=0,\mu=0$

**Set 3**

$$u_3=\mp\frac{\rho}{\sigma}+\frac{15d^4kw\delta}{\sigma(\xi_3+\xi_0)^2}+\frac{120d^6k^3\gamma}{\sigma(\xi_3+\xi_0)^3},\xi_3=\frac{k}{\beta}\left(x+\frac{1}{\Gamma(\beta)}\right)^{\beta}.$$

If we select $\sigma=\rho=d=\delta=k=w=\gamma=1,\xi_0=0$. The numerical simulation of rational function $u_3$ is shown in Figure 5.

## 3.2 Using the $G'/(bG'+G+a)$-expansion method

We assume that Eq. 10 has the following solutions:

$$u=a_0+a_1F+a_2F^2+a_3F^3, \qquad (12)$$

where $a_0,a_1,a_2$ and $a_3$ are constants to be determined later; if we select $b=1$, substituting Eqs 9, 12 into Eq. 10 and setting the coefficients of $F^i$ zero yields

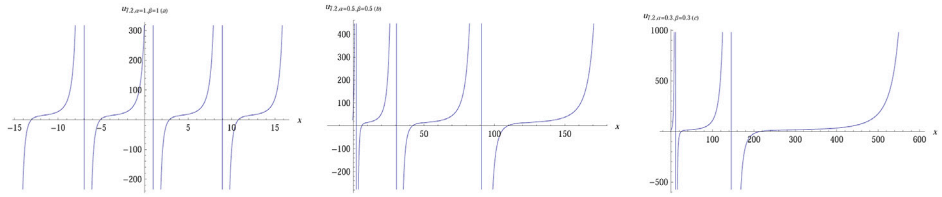

**FIGURE 11**
Changes in the waveform of $u_{7,2}$ with different values of $\alpha, \beta$.

$$F^0:\ \frac{1}{2}a_0(2w + 2k\rho + k\sigma a_0) = A + k^2\mu((w\delta(\lambda - 2\mu) - \mu + k^2\gamma(\lambda^2 + 2\mu - 6\lambda\mu + 6\mu^2))a_1 + 2\mu((w\delta + 3k^2\gamma(\lambda - 2\mu))a_2 + 3k^2\gamma\mu a_3)),$$

$$F:\ (-w(-1 + k^2\delta(\lambda^2 + 2\mu - 6\lambda\mu + 6\mu^2)) + k(k(\lambda - 2\mu)\mu - k^3\gamma(\lambda^3 - 14\lambda^2\mu - 8\mu^2(2 + 3\mu) + 4\lambda\mu(2 + 9\mu)) + \rho + \sigma a_0))a_1 = 2k^2\mu((3w\delta(\lambda - 2\mu) - \mu + k^2\gamma(7\lambda^2 - 36\lambda\mu + 4\mu(2 + 9\mu)))a_2 + 3(w\delta + 6k^2\gamma(\lambda - 2\mu))\mu a_3),$$

$$F^2:\ (w(1 - 4k^2\delta(\lambda^2 + 2\mu - 6\lambda\mu + 6\mu^2)) + k(2k(\lambda - 2\mu)\mu - 4k^3\gamma(2\lambda^3 - 25\lambda^2\mu - 2\mu^2(13 + 21\mu) + \lambda\mu(13 + 63\mu)) + \rho + \sigma a_0))a_2 + \frac{1}{2}k(2k(\lambda - \mu - 1)(3w\delta(\lambda - 2\mu) - \mu + k^2\gamma(7\lambda^2 - 36\lambda\mu + 4\mu(2 + 9\mu)))a_1 + \sigma a_1^2 - 6k\mu(5w\delta(\lambda - 2\mu) - \mu + k^2\gamma(19\lambda^2 - 96\lambda\mu + 4\mu(5 + 24\mu)))a_3) = 0,$$

$$F^3:\ k(2k(-1 + \lambda - \mu)(5w\delta(\lambda - 2\mu) - \mu + k^2\gamma(19\lambda^2 - 96\lambda\mu + 4\mu(5 + 24\mu)))a_2 + a_1(-2kw\delta(1 - \lambda + \mu)^2 - 12k^3\gamma(\lambda - 2\mu)(1 - \lambda + \mu)^2 + \sigma a_2)) + (w(1 - 9k^2\delta(\lambda^2 + 2\mu - 6\lambda\mu + 6\mu^2)) + k(3k(\lambda - 2\mu)\mu - 3k^3\gamma(9\lambda^3 - 110\lambda^2\mu - 8\mu^2(14 + 23\mu) + 4\lambda\mu(14 + 69\mu)) + \rho + \sigma a_0))a_3 = 0,$$

$$F^4:\ k(12k(w\delta + 9k^2\gamma(\lambda - 2\mu))(1 - \lambda + \mu)^2 a_2 - \sigma a_2^2 - 6k(-1 + \lambda - \mu)(7w\delta(\lambda - 2\mu) - \mu + k^2\gamma(37\lambda^2 - 186\lambda\mu + 2\mu(19 + 93\mu)))a_3 - 2a_1(6k^3\gamma(-1 + \lambda - \mu)^3 + \sigma a_3)) = 0,$$

$$F^5:\ k(-12k(w\delta + 12k^2\gamma(\lambda - 2\mu))(1 - \lambda + \mu)^2 a_3 + a_2(24k^3\gamma(-1 + \lambda - \mu)^3 + \sigma a_3)) = 0,$$

$$F^6:\ ka_3(120k^3\gamma(-1 + \lambda - \mu)^3 + \sigma a_3) = 0.$$

We can deduce the following solutions with the aid of mathematical software.

### Case 1:

$$a_0 = \frac{4T}{\delta\sigma k} + \frac{60kT^2(\lambda^2 + 2\mu^2 - \lambda + 2\mu - 3\lambda\mu)}{\sigma} + \frac{\rho}{\varepsilon\sigma} + \frac{6kT\varepsilon(\lambda^2 + 10\mu^2 + 6\mu - 10\lambda\mu)}{\sigma},$$

$$a_1 = \frac{60k(1 - \lambda + \mu)\left[\varepsilon T(\lambda - 2\mu) + \gamma k^2(2\mu + 6\mu^2 + \lambda^2 - 6\lambda\mu)\right]}{\sigma}, T = \sqrt{\frac{\mu^2}{\Delta}},$$

$$a_2 = -\frac{60\gamma k^3(1 - \lambda + \mu)^2(\varepsilon\sqrt{\Delta} - 3\lambda + 6\mu)}{\sigma}, a_3 = \frac{120\gamma k^3(1 - \lambda + \mu)^3}{\sigma}, \Delta = \lambda^2 - 4\mu,$$

$$A = \frac{k}{\sigma}\left(\frac{8\gamma\mu}{\delta^2} - \frac{18\mu^3}{\gamma} - \frac{4\rho T}{\varepsilon\delta k} - \frac{\rho^2}{2}\right), w = \frac{4T}{\delta\varepsilon}, k = \varepsilon\sqrt{\frac{\mu}{-\gamma\Delta}}, \varepsilon = \pm 1.$$

### Case 2:

$$a_0 = \frac{k\Delta T}{\sigma}\left(-\frac{12\gamma}{\delta\mu} + \frac{15}{47}\right) + \frac{\rho}{\varepsilon\sigma} + \frac{15Tk(\lambda^2 - 12\lambda\mu + 8\mu + 12\mu^2)}{47\varepsilon\sigma} + \frac{60k^3\gamma}{\sigma}(\lambda^3 - 3\lambda^2\mu + 3\lambda\mu + 6\mu^2 - 2\mu^3),$$

$$a_1 = \frac{180k(1 - \lambda + \mu)\left[\varepsilon T(\lambda - 2\mu) + 47\gamma k^2(2\mu^2 - 2\mu + \lambda^2 - 2\lambda\mu)\right]}{47\sigma}, \mathrm{T} = \sqrt{\frac{\mu^2}{\Delta}},$$

$$a_2 = -\frac{180\gamma k^3(1 - \lambda + \mu)^2(\varepsilon\sqrt{\Delta} - \lambda + 2\mu)}{\sigma}, a_3 = \frac{120\gamma k^3(1 - \lambda + \mu)^3}{\sigma}, \Delta = \lambda^2 - 4\mu,$$

$$A = \frac{k}{\sigma}\left(\frac{72\gamma\mu}{47\delta^2} - \frac{1800\mu^3}{103823\gamma} - \frac{12\rho T}{47\varepsilon\delta k} - \frac{\rho^2}{2}\right),$$

$$w = \frac{12T}{47\delta\varepsilon}, k = \varepsilon\sqrt{\frac{\mu}{-47\gamma\Delta}}, \varepsilon = \pm 1.$$

### Case 3:

$$a_0 = \frac{4Tk}{73\sigma}\left[\frac{4}{\delta k^2} + 5\Delta + 5\varepsilon(\lambda^2 + 8\mu - 12\lambda\mu + 12\mu^2)\right] + \frac{30\gamma k^3}{\sigma}\left[3\lambda^3 + 2\lambda\mu(3\mu - 5) - 8\lambda^2\mu - 4\mu^2(\mu - 5)\right] + \frac{\rho}{\varepsilon\sigma},$$

$$a_1 = \frac{120k(1 - \lambda + \mu)\left[2\varepsilon T(\lambda - 2\mu) + 73\gamma k^2(3\mu^2 - 5\mu + 2\lambda^2 - 3\lambda\mu)\right]}{73\sigma},$$

$$a_2 = -\frac{60\gamma k^3(1 - \lambda + \mu)^2(4\varepsilon\sqrt{\Delta} - 3\lambda + 6\mu)}{\sigma}, a_3 = \frac{120\gamma k^3(1 - \lambda + \mu)^3}{\sigma}, T = \sqrt{\frac{\mu^2}{\Delta}},$$

$$A = \frac{k}{\sigma}\left(\frac{128\gamma\mu}{73\delta^2} - \frac{4050\mu^3}{389017\gamma} - \frac{16\rho T}{73\varepsilon\delta k} - \frac{\rho^2}{2}\right), w = \frac{16\varepsilon T}{73\delta}, k = \varepsilon\sqrt{\frac{\mu}{-73\gamma\Delta}}, \Delta = \lambda^2 - 4\mu, \varepsilon = \pm 1.$$

### Case 4:

$$a_0 = \frac{4T}{\sigma}\left[\frac{1}{\delta k} + \varepsilon k(\lambda^2 + 11\mu - 15\lambda\mu + 15\mu^2)\right] + \frac{\rho}{\sigma\varepsilon} + \frac{60T^2k}{\sigma}(\lambda^2 + 2\mu^2 - 3\lambda\mu + 2\mu - \lambda),$$

$$a_1 = \frac{60k(1 - \lambda + \mu)\left[T\varepsilon(\lambda - 2\mu) + k^2\gamma(\lambda^2 - 6\lambda\mu + 2\mu + 6\mu^2)\right]}{\sigma},$$

$$a_2 = \frac{60k(1 - \lambda + \mu)^2(T\varepsilon\Delta + 3\lambda\mu - 6\mu^2)}{\Delta\sigma},$$

$$a_3 = \frac{120\gamma k^3(1 - \lambda + \mu)^3}{\sigma}, \Delta = \lambda^2 - 4\mu,$$

$$A = \frac{k}{\sigma}\left(\frac{8\gamma\mu}{\delta^2} - \frac{8\mu^3}{\gamma} - \frac{4\rho T}{\varepsilon\delta k} - \frac{\rho^2}{2}\right),$$

$$w = \frac{4T}{\delta\varepsilon}, k = \varepsilon\sqrt{\frac{\mu}{\gamma\Delta}}, T = \sqrt{\frac{\mu^2}{-\Delta}}, \varepsilon = \pm 1.$$

We can determine the following solutions.

**Family 4** $\Delta = \lambda^2 - 4\mu > 0$

For case 1, we have

**Set 4**

$$u_4 = \frac{4T}{\delta\sigma k} + \frac{60kT^2(\lambda^2 + 2\mu^2 - \lambda + 2\mu - 3\lambda\mu)}{\sigma} + \frac{\rho}{\varepsilon\sigma} + \frac{6kT\varepsilon(\lambda^2 + 10\mu^2 + 6\mu - 10\lambda\mu)}{\sigma} + \frac{60k(1-\lambda+\mu)\left[\varepsilon T(\lambda - 2\mu) + \gamma k^2(2\mu + 6\mu^2 + \lambda^2 - 6\lambda\mu)\right]}{\sigma}F_1(\xi_4) - \frac{60\gamma k^3(1-\lambda+\mu)^2\left(\varepsilon\sqrt{\Delta} - 3\lambda + 6\mu\right)}{\sigma}F_1^2(\xi_4) + \frac{120\gamma k^3(1-\lambda+\mu)^3}{\sigma}F_1^3(\xi_4).$$

where

$$F_1(\xi_4) = \frac{[\lambda(p_2 - p_1) - \sqrt{\Delta}(p_2 + p_1)]sinh\left(\frac{\sqrt{\Delta}}{2}\xi_4\right) + [\lambda(p_2 + p_1) - \sqrt{\Delta}(p_2 - p_1)]cosh\left(\frac{\sqrt{\Delta}}{2}\xi_4\right)}{[(\lambda - 2)(p_2 - p_1) - \sqrt{\Delta}(p_2 + p_1)]sinh\left(\frac{\sqrt{\Delta}}{2}\xi_4\right) + [(\lambda - 2)(p_2 + p_1) - \sqrt{\Delta}(p_2 - p_1)]cosh\left(\frac{\sqrt{\Delta}}{2}\xi_4\right)},$$

$$\xi_4 = \frac{\varepsilon}{\beta}\sqrt{\frac{\mu}{-\gamma\Delta}}\left(x + \frac{1}{\Gamma(\beta)}\right)^{\beta} + \frac{4\varepsilon}{\alpha\delta}\sqrt{\frac{\mu^2}{\lambda^2 - 4\mu}}\left(t + \frac{1}{\Gamma(\alpha)}\right)^{\alpha},$$
$$\Delta = \lambda^2 - 4\mu, k = \varepsilon\sqrt{\frac{\mu}{-\gamma\Delta}}, T = \sqrt{\frac{\mu^2}{\Delta}}.$$

The numerical simulation of $u_4$ is shown in Figure 6, where we select

$$\lambda = -2, \mu = -1, \varepsilon = 1, \gamma = 1, \delta = 1, \rho = 1, \sigma = 1, p_1 = 1, p_2 = 2,$$
$$b = 1, k = \sqrt{2}/4, w = \sqrt{2}, a_3 = 30\sqrt{2}, a_2 = 30, a_1 = -15\sqrt{2},$$
$$a_0 = -4, A = \frac{19}{4\sqrt{2}} - \sqrt{2}, \Delta = 8, T = \frac{1}{2\sqrt{2}}.$$

For case 2, we have

**Set 5**

$$u_5 = \frac{k\Delta T}{\sigma}\left(\frac{15}{47} - \frac{12\gamma}{\delta\mu}\right) + \frac{15Tk(\lambda^2 - 12\lambda\mu + 8\mu + 12\mu^2)}{47\varepsilon\sigma} + \frac{60k^3\gamma}{\sigma}(\lambda^3 - 3\lambda^2\mu + 3\lambda\mu + 6\mu^2 - 2\mu^3) + \frac{\rho}{\varepsilon\sigma} + \frac{180k(1-\lambda+\mu)\left[\varepsilon T(\lambda - 2\mu) + 47\gamma k^2(2\mu^2 - 2\mu + \lambda^2 - 2\lambda\mu)\right]}{47\sigma}F_1(\xi_5) - \frac{180\gamma k^3(1-\lambda+\mu)^2\left(\varepsilon\sqrt{\Delta} - \lambda + 2\mu\right)}{\sigma}F_1^2(\xi_5) + \frac{120\gamma k^3(1-\lambda+\mu)^3}{\sigma}F_1^3(\xi_5).$$

where

$$F_1(\xi_5) = \frac{[\lambda(p_2 - p_1) - \sqrt{\Delta}(p_2 + p_1)]\sinh\left(\frac{\sqrt{\Delta}}{2}\xi_5\right) + [\lambda(p_2 + p_1) - \sqrt{\Delta}(p_2 - p_1)]\cosh\left(\frac{\sqrt{\Delta}}{2}\xi_5\right)}{[(\lambda - 2)(p_2 - p_1) - \sqrt{\Delta}(p_2 + p_1)]\sinh\left(\frac{\sqrt{\Delta}}{2}\xi_5\right) + [(\lambda - 2)(p_2 + p_1) - \sqrt{\Delta}(p_2 - p_1)]\cosh\left(\frac{\sqrt{\Delta}}{2}\xi_5\right)},$$

$$\xi_5 = \frac{\varepsilon}{\beta}\sqrt{\frac{\mu}{-47\gamma\Delta}}\left(x + \frac{1}{\Gamma(\beta)}\right)^{\beta} + \frac{12\varepsilon}{47\delta\alpha}\sqrt{\frac{\mu^2}{\lambda^2 - 4\mu}}\left(t + \frac{1}{\Gamma(\alpha)}\right)^{\alpha},$$
$$\Delta = \lambda^2 - 4\mu, k = \sqrt{\frac{\mu}{-47\gamma\Delta}}, T = \sqrt{\frac{\mu^2}{\Delta}}.$$

The numerical simulation of $u_5$ is shown in Figure 7, where we select

$$\lambda = -2, \mu = -1, \varepsilon = 1, \gamma = 1, \delta = 1, \rho = 1\big/\sqrt{47}, \sigma = 1\big/\sqrt{47}, p_1$$
$$= 1, p_2 = 2, b = 1, w = \frac{3\sqrt{2}}{47}, k = \frac{1}{2\sqrt{94}}, a_3 = \frac{30\sqrt{2}}{47}, a_2 = \frac{90}{47}, a_1$$
$$= \frac{45\sqrt{2}}{47}, a_0 = \frac{596}{47}, A = -\frac{369721}{415292\sqrt{2}}, \Delta = 8, T = \frac{1}{2\sqrt{2}}.$$

For case 3, we have

**Set 6**

$$u_6 = \frac{4Tk}{73\sigma}\left[\frac{4}{\delta k^2} + 5\Delta + 5\varepsilon(\lambda^2 + 8\mu - 12\lambda\mu + 12\mu^2)\right] + \frac{30\gamma k^3}{\sigma}\left[3\lambda^3 + 2\lambda\mu(3\mu - 5) - 8\lambda^2\mu - 4\mu^2(\mu - 5)\right] + \frac{\rho}{\varepsilon^3\sigma} + \frac{120k(1-\lambda+\mu)\left[2\varepsilon T(\lambda - 2\mu) + 73\gamma k^2(3\mu^2 - 5\mu + 2\lambda^2 - 3\lambda\mu)\right]}{73\sigma}F_1(\xi_6) - \frac{60\gamma k^3(1-\lambda+\mu)^2\left(4\varepsilon\sqrt{\Delta} - 3\lambda + 6\mu\right)}{\sigma}F_1^2(\xi_6) + \frac{120\gamma k^3(1-\lambda+\mu)^3}{\sigma}F_1^3(\xi_6).$$

where

$$F_1(\xi_6) = \frac{[\lambda(p_2 - p_1) - \sqrt{\Delta}(p_2 + p_1)]\sinh\left(\frac{\sqrt{\Delta}}{2}\xi_6\right) + [\lambda(p_2 + p_1) - \sqrt{\Delta}(p_2 - p_1)]\cosh\left(\frac{\sqrt{\Delta}}{2}\xi_6\right)}{[(\lambda - 2)(p_2 - p_1) - \sqrt{\Delta}(p_2 + p_1)]\sinh\left(\frac{\sqrt{\Delta}}{2}\xi_6\right) + [(\lambda - 2)(p_2 + p_1) - \sqrt{\Delta}(p_2 - p_1)]\cosh\left(\frac{\sqrt{\Delta}}{2}\xi_6\right)},$$

$$\xi_6 = \frac{\varepsilon}{\beta}\sqrt{\frac{\mu}{-73\gamma\Delta}}\left(x + \frac{1}{\Gamma(\beta)}\right)^{\beta} + \frac{16\varepsilon}{73\delta\alpha}\sqrt{\frac{\mu^2}{\lambda^2 - 4\mu}}\left(t + \frac{1}{\Gamma(\alpha)}\right)^{\alpha},$$
$$\Delta = \lambda^2 - 4\mu, k = \varepsilon\sqrt{\frac{\mu}{-73\gamma\Delta}}, T = \sqrt{\frac{\mu^2}{\Delta}}, \varepsilon = \pm 1.$$

The numerical simulation of $u_6$ is shown in Figure 8, where we select

$$\lambda = \sqrt{5}, \mu = 1, \varepsilon = -1, \gamma = -1, \delta = 1, \rho = \frac{1}{73\sqrt{73}}, \sigma = \frac{1}{73\sqrt{73}},$$
$$p_1 = 1, p_2 = 2, k = -\frac{1}{\sqrt{73}}, a_3 = -120(-2 + \sqrt{5})^3,$$
$$a_2 = 60(-78 + 35\sqrt{5}), a_1 = 1560 - 720\sqrt{5},$$
$$a_0 = -1409 + 90\sqrt{5}, w = -\frac{16}{73}, \Delta = 1, T = 1, A = \frac{1358461}{10658}.$$

**Family 5** $\Delta = \lambda^2 - 4\mu < 0$ For case 4, we have

**Set 7**

$$u_7 = \frac{4T}{\sigma}\left[\frac{1}{\delta k} + \varepsilon k(\lambda^2 + 11\mu - 15\lambda\mu + 15\mu^2)\right] + \frac{\rho}{\sigma\varepsilon} + \frac{60T^2k}{\sigma}(\lambda^2 + 2\mu^2 - 3\lambda\mu + 2\mu - \lambda) + \frac{60k(1-\lambda+\mu)\left[T\varepsilon(\lambda - 2\mu) + k^2\gamma(\lambda^2 - 6\lambda\mu + 2\mu + 6\mu^2)\right]}{\sigma}F_2(\xi_7) + \frac{60k(1-\lambda+\mu)^2(T\varepsilon\Delta + 3\lambda\mu - 6\mu^2)}{\Delta\sigma}F_2^2(\xi_7) + \frac{120\gamma k^3(1-\lambda+\mu)^3}{\sigma}F_2^3(\xi_7).$$

where

$$F_2(\xi_7) = \frac{(\lambda p_1 - \sqrt{-\Delta}\,p_2)\cos\left(\frac{\sqrt{-\Delta}}{2}\xi_7\right) + (\lambda p_2 + \sqrt{-\Delta}\,p_1)\sin\left(\frac{\sqrt{-\Delta}}{2}\xi_7\right)}{[(\lambda - 2)p_1 - \sqrt{-\Delta}\,p_2]\cos\left(\frac{\sqrt{-\Delta}}{2}\xi_7\right) + [(\lambda - 2)p_2 + \sqrt{-\Delta}\,p_1]\sin\left(\frac{\sqrt{-\Delta}}{2}\xi_7\right)}$$

$$\xi_7 = \frac{\varepsilon}{\beta}\sqrt{\frac{\mu}{\gamma\Delta}}\left(x + \frac{1}{\Gamma(\beta)}\right)^{\beta} + \frac{4\varepsilon}{\delta\alpha}\sqrt{\frac{\mu^2}{4\mu - \lambda^2}}\left(t + \frac{1}{\Gamma(\alpha)}\right)^{\alpha}.$$

$$\Delta = \lambda^2 - 4\mu, w = \frac{4T\varepsilon}{\delta}, k = \varepsilon\sqrt{\frac{\mu}{\gamma\Delta}}, T = \sqrt{\frac{\mu^2}{-\Delta}}.$$

The numerical simulation of $u_7$ with the fractional order is shown in Figure 9, where we select

$$\lambda = 2, \mu = 2, \varepsilon = -1, \gamma = -2, \delta = 1, \rho = 1, \sigma = 1, w = -4,$$
$$k = -1/2, p_1 = 1, p_2 = 2, a_3 = 30, a_2 = -60, a_1 = 60, a_0 = -17,$$
$$A = \frac{17}{4}, \Delta = -4, T = 1.$$

Clearly, if we select the special value of $p_1, p_2$ in $F_1, F_2$, we can obtain the tanh, coth, tan, and cot-type solutions; without loss of generality, we select

$$\lambda = 4, \mu = 2, \varepsilon = 1, \gamma = -2, \delta = 1, \rho = 2, \sigma = 2, b = 1, k = \frac{1}{2\sqrt{2}},$$
$$w = 2\sqrt{2}, \Delta = 8, T = \frac{1}{\sqrt{2}}, a_3 = \frac{15}{2\sqrt{2}}, a_2 = \frac{15}{2}, a_1 = -\frac{15}{\sqrt{2}},$$
$$a_0 = -4, A = \frac{19}{2\sqrt{2}} - 2\sqrt{2}.$$

Thus, we obtain the following solutions:

$$F_{1.1} = -\sqrt{2}\tanh\left[\frac{1}{2\beta}\left(x + \frac{1}{\Gamma(\beta)}\right)^{\beta} + \frac{4}{\alpha}\left(t + \frac{1}{\Gamma(\alpha)}\right)^{\alpha}\right], (1 + \sqrt{2})p_1 = (1 - \sqrt{2})p_2.$$

$$F_{1.2} = -\sqrt{2}\coth\left[\frac{1}{2\beta}\left(x + \frac{1}{\Gamma(\beta)}\right)^{\beta} + \frac{4}{\alpha}\left(t + \frac{1}{\Gamma(\alpha)}\right)^{\alpha}\right], (\sqrt{2} - 1)p_1 = (\sqrt{2} - 1)p_2. u_{4.1} = -4 - \frac{15}{\sqrt{2}}F_{1.1} + \frac{15}{2}F_{1.1}^2 + \frac{15}{2\sqrt{2}}F_{1.1}^3,$$
$$u_{4.2} = -4 - \frac{15}{\sqrt{2}}F_{1.2} + \frac{15}{2}F_{1.2}^2 + \frac{15}{2\sqrt{2}}F_{1.2}^3.$$

If we select

$$w = \frac{5}{2}, k = \frac{1}{4}\sqrt{\frac{5}{2}}, \lambda = 1, \mu = 5/4, \varepsilon = 1, \gamma = -2, \delta = 1, \rho = 1,$$
$$\sigma = 1, w = \frac{5}{2}, p_1 = 1, p_2 = 2, \Delta = -4, T = \frac{5}{8}, a_3 = -\frac{9375}{512}\sqrt{\frac{5}{2}},$$
$$a_2 = \frac{24375}{512}\sqrt{\frac{5}{2}}, a_1 = -\frac{25125}{512}\sqrt{\frac{5}{2}}, a_0 = 1 + \frac{13893}{512}\sqrt{\frac{5}{2}},$$
$$A = -\frac{5}{2} - \frac{203}{64}\sqrt{\frac{5}{2}}.$$

Thus,

$$F_{2.1} = \frac{3}{5} - \frac{4}{5}\tan\left[\frac{1}{4\beta}\sqrt{\frac{5}{2}}\left(x + \frac{1}{\Gamma(\beta)}\right)^{\beta} + \frac{5}{\alpha}\left(t + \frac{1}{\Gamma(\alpha)}\right)^{\alpha}\right], p_2 = 2p_1,$$

$$F_{2.2} = \frac{3}{5} + \frac{4}{5}cot\left[\frac{1}{4\beta}\sqrt{\frac{5}{2}}\left(x + \frac{1}{\Gamma(\beta)}\right)^{\beta} + \frac{5}{\alpha}\left(t + \frac{1}{\Gamma(\alpha)}\right)^{\alpha}\right], p_1 = -2p_2.$$

We have

$$u_{7.1} = 1 + \frac{13893}{512}\sqrt{\frac{5}{2}} - \frac{25125}{512}\sqrt{\frac{5}{2}}F_{1.1} + \frac{24375}{512}\sqrt{\frac{5}{2}}F_{1.1}^2 - \frac{9375}{512}\sqrt{\frac{5}{2}}F_{1.1}^3,$$
$$u_{7.2} = 1 + \frac{13893}{512}\sqrt{\frac{5}{2}} - \frac{25125}{512}\sqrt{\frac{5}{2}}F_{2.2} + \frac{24375}{512}\sqrt{\frac{5}{2}}F_{2.2}^2 - \frac{9375}{512}\sqrt{\frac{5}{2}}F_{2.2}^3.$$

The simulation of $u_{4.1}$ is shown in Figure 10.

## 3.3 Results and discussion

After utilizing the modified sub-equation method and the new G'/(bG'+G+a)-expansion method, we obtain many types of exact solutions of Eq. 1, and some structures of these solutions are simulated in Figures 1–10. Visualization can help us better understand the dynamic behavior and propagation property of these solutions. For example, the bell-shape-like solitary wave solution of Eq. 1 is shown in Figure 1, and we find that there are two asymptotes on either side of the peak for $u_{2.1.1}$, while the bell-shape soliton solution has only one. The shape of trigonometric function solutions $u_{2.1.2}$ has a break when $x \in (46, 48)$, which is shown in Figure 2. The same phenomena happen for $u_3$ and $u_6$ which are simulated in Figures 5, 8. The simulations of periodic solutions $u_{2.2.1}$, $u_{2.2.2}$, and $u_7$ are shown in Figures 3, 4, 9 for $\alpha = \beta = 1$ or $0 < \alpha, \beta < 1$. We can find that the waveform of a single period widens as the order decreases, and the changes of $u_{7.2}$ are simulated in Figure 11. The kink soliton solution $u_4$ and the solitary wave solution $u_5$ for the fractional order are simulated in Figures 6, 7. From Figure 10, we find the solution $u_{4.1}$ has one peak, one valley, and two asymptotes. These different propagation patterns can probably explain the different phenomena for this model.

# 4 Conclusion

In conclusion, many types of new exact solutions for the Atangana fractional GBBM–Burgers equation with the dissipative term have been found after utilizing the modified sub-equation method and the new *G'/(bG' + G + a)*-expansion method. Some propagation behavioral patterns of these solutions are discussed and simulated, the graphs of which show that these solitary wave solutions, trigonometric function periodic solutions, and rational function solutions are propagated through different patterns. The two efficient and significant methods can be used for many other nonlinear models such as the vmKdV equation, Ginzburg–Landau equation, and NLS-KDV equation. However, it is still worth researching whether the method can be used in a system with high dimensions and high order. Finally, all these solutions obtained in the present article have been checked by mathematical software.

# Data availability statement

The original contributions presented in the study are included in the article/Supplementary Material; further inquiries can be directed to the corresponding author.

## Author contributions

BH: completed the study, carried out the tests, and drafted the manuscript.

## Funding

This work is supported by the practical innovation training program projects for the university students of Jiangsu Province (Grant No. 202211276054Y), natural science research projects of Institutions in Jiangsu Province (Grant No. 18KJB110013), and the Nanjing Institute of Technology (Grant Nos. ZKJ201513 and YZKC2019086).

## Conflict of interest

The author declares that the research was conducted in the absence of any commercial or financial relationships that could be construed as a potential conflict of interest.

## Publisher's note

All claims expressed in this article are solely those of the authors and do not necessarily represent those of their affiliated organizations, or those of the publisher, the editors, and the reviewers. Any product that may be evaluated in this article, or claim that may be made by its manufacturer, is not guaranteed or endorsed by the publisher.

## References

1. Oldham KB, Spanier J. *The fractional calculus*. New York: Academic (1974).

2. He JH, Jiao ML, He CH. Homotopy perturbation method for fractal Duffing oscillator with arbitrary conditions. *Fractals* (2022). doi:10.1142/S0218348X22501651

3. Khan RA, Li Y, Jarad F. Exact analytical solutions of fractional order telegraph equations via triple Laplace transform. *Discrete & Continuous Dynamical Systems-S* (2018) 14(7):2387–11. doi:10.3934/dcdss.2020427

4. Alshammari S, Iqba N, Yar M. Analytical investigation of nonlinear fractional Harry Dym and Rosenau-Hyman equation via a novel transform. *J Funct Spaces* (2022) 2022:1–12. doi:10.1155/2022/8736030

5. Almutairi A, El-Metwally H, Sohaly MA, Elbaz IM. Lyapunov stability analysis for nonlinear delay systems under random effects and stochastic perturbations with applications in finance and ecology. *Adv Differ Equ* (2021) 2021(1):186–32. doi:10.1186/s13662-021-03344-6

6. He JH. Seeing with a single scale is always unbelieving: From magic to two-scale fractal. *Therm Sci* (2021) 25(2B):1217–9. doi:10.2298/tsci2102217h

7. Zhang RF, Bilige S. Bilinear neural network method to obtain the exact analytical solutions of nonlinear partial differential equations and its application to p-gBKP equation. *Nonlinear Dyn* (2019) 95(4):3041–8. doi:10.1007/s11071-018-04739-z

8. Tavazoei MS, Haeri M, Jafari S, Bolouki S, Siami M. Some applications of fractional calculus in suppression of chaotic oscillations. *IEEE Trans Ind Electron* (2008) 55(11):4094–101. doi:10.1109/tie.2008.925774

9. Korn P. A Regularity-Aware algorithm for variational data assimilation of an idealized coupled Atmosphere-Ocean Model. *J Sci Comput* (2018) 79(2):748–86. doi:10.1007/s10915-018-0871-y

10. Yokus A, Baskonus HM. Dynamics of traveling wave solutions arising in fiber optic communication of some nonlinear models. *Soft Comput* (2022) 2022:1–10. doi:10.1007/s00500-022-07320-4

11. Abdelwahed HG, El-Shewy EK, Abdelrahman MAE, Alsarhana A. On the physical nonlinear (n+1)-dimensional Schrödinger equation applications. *Results Phys* (2021) 21:103798. doi:10.1016/j.rinp.2020.103798

12. Samei ME, Karimi L, Kaabar MKA. To investigate a class of multi-singular pointwise defined fractional $ q $–integro-differential equation with applications. *AIMS Math* (2022) 7(5):7781–816. doi:10.3934/math.2022437

13. Matveev VA, Salle MA. *Darboux transformations and solitons*. Berlin, Heidelberg: Springer-Verlag (1991).

14. Lu DC, Hong BJ. Bäcklund transformation and n-soliton-like solutions to the combined KdV-Burgers equation with variable coefficients. *Int J Nonlinear Sci* (2006) 1(2):3–10. http://www.worldacademicunion.com/journal/1749-3889-3897IJNS/IJNSVol2No1Paper1.pdf

15. Qi FH, Li S, Li ZH, Wang P. Multiple lump solutions of the (2+1)-dimensional sawada-kotera -like equation. *Front Phys* (2022) 10:1041100. doi:10.3389/fphy.2022.1041100

16. Bashar MH, Islam SMR. Exact solutions to the (2+1)-Dimensional Heisenberg ferromagnetic spin chain equation by using modified simple equation and improve F-expansion methods. *Phys Open* (2020) 5:100027. doi:10.1016/j.physo.2020.100027

17. Lu DC, Hong BJ, Tian LX. New explicit exact solutions for the generalized coupled Hirota-Satsuma KdV system. *Comput Math Appl* (2007) 53:1181–90. doi:10.1016/j.camwa.2006.08.047

18. Kundu RP, Fahim M, Islam ME, Akbar MA. The sine-Gordon expansion method for higher- dimensional NLEEs and parametric analysis. *Heliyon* (2021) 7(3):e06459. doi:10.1016/j.heliyon.2021.e06459

19. Hong BJ. New Jacobi elliptic functions solutions for the variable-coefficient mKdV equation. *Appl Math Comput* (2009) 215(8):2908–13. doi:10.1016/j.amc.2009.09.035

20. Mohanty SK, Kravchenko OV, Dev AN. Exact traveling wave solutions of the Schamel Burgers' equation by using generalized-improved and generalized G′G expansion methods. *Results Phys* (2022) 33:105124. doi:10.1016/j.rinp.2021.105124

21. Siddique I, Jaradat MMM, Zafar A, Bukht Mehdi K, Osman M. Exact traveling wave solutions for two prolific conformable M-Fractional differential equations via three diverse approaches. *Results Phys* (2021) 33:104557. doi:10.1016/j.rinp.2021.104557

22. Ismael HF, Bulut H, Baskonus HM. Optical soliton solutions to the Fokas–Lenells equation via sine-Gordon expansion method and (m+(G'/G))-expansion method. *Pramana* (2020) 94(1):1–9. doi:10.1007/s12043-019-1897-x

23. Mohyud-Din ST, Bibi S. Exact solutions for nonlinear fractional differential equations using G′G2-expansion method-expansion method. *Alexandria Eng J* (2018) 57(2):1003–8. doi:10.1016/j.aej.2017.01.035

24. Fei J, Ma Z, Cao W. Soliton molecules of new (2+1)-dimensional Burgers-type equation. *Eur Phys J Plus* (2022) 137(1):104–11. doi:10.1140/epjp/s13360-021-02306-x

25. Fan EG. Two new applications of the homogeneous balance method. *Phys Lett A* (2000) 265:353–7. doi:10.1016/s0375-9601(00)00010-4

26. Ma WX, Osman MS, Arshed S, Raza N, Srivastava H. Practical analytical approaches for finding novel optical solitons in the single-mode fibers. *Chin J Phys* (2021) 72:475–86. doi:10.1016/j.cjph.2021.01.015

27. Ablowitz MJ, Solitons PAC. *Nonlinear evolution equations and inverse scattering*. New York: Cambridge University Press (1991).

28. Nass AM. Lie symmetry analysis and exact solutions of fractional ordinary differential equations with neutral delay. *Appl Math Comput* (2019) 347:370–80. doi:10.1016/j.amc.2018.11.002

29. Yue C, Lu DC, Khater MMA, Abdel-Aty AH, Alharbi W, Attia RAM. On explicit wave solutions of the fractional nonlinear DSW system via the modified Khater method. *Fractals* (2020) 28(8):2040034. doi:10.1142/s0218348x20400344

30. He JH, Elagan SK, Li ZB. Geometrical explanation of the fractional complex transform and derivative chain rule for fractional calculus. *Phys Lett A* (2012) 376(4):257–9. doi:10.1016/j.physleta.2011.11.030

31. He JH. Fractal calculus and its geometrical explanation. *Results Phys* (2018) 10:272–6. doi:10.1016/j.rinp.2018.06.011

32. Yu F, Yu Q, Chen H, Kong X, Mokbel AAM, Cai S, et al. Dynamic analysis and audio encryption application in IoT of a multi-scroll fractional-order memristive hopfield neural network. *Fractal Fract* (2022) 6(7):370. doi:10.3390/fractalfract6070370

33. Hong BJ, Lu DC, Chen W. Exact and approximate solutions for the fractional Schrödinger equation with variable coefficients. *Adv Differ Equ* (2019) 2019(370): 370–10. doi:10.1186/s13662-019-2313-z

34. Biswas A. Conservation laws for optical solitons with anti-cubic and generalized anticubic nonlinearities. *Optik* (2019) 176:198–201. doi:10.1016/j.ijleo.2018.09.074

35. Haq A. Partial-approximate controllability of semi-linear systems involving two Riemann-Liouville fractional derivatives. *Chaos Solitons Fractals* (2022) 157: 111923. doi:10.1016/j.chaos.2022.111923

36. Caputo M. Linear models of dissipation whose Q is almost frequency independent: Part II. *Geophys J Int* (1967) 13:529–39. doi:10.1111/j.1365-246x.1967.tb02303.x

37. Guner O, Atik H, Kayyrzhanovich AA. New exact solution for space-time fractional differential equations via (G'/G)-expansion method. *Optik* (2017) 130: 696–701. doi:10.1016/j.ijleo.2016.10.116

38. He JH. A tutorial review on fractal spacetime and fractional calculus. *Int J Theor Phys (Dordr)* (2014) 53:3698–718. doi:10.1007/s10773-014-2123-8

39. Tajadodi H. A Numerical approach of fractional advection-diffusion equation with Atangana Baleanu derivative. *Chaos Solitons Fractals* (2020) 130:109527. doi:10.1016/j.chaos.2019.109527

40. Yao SW, Manzoor R, Zafar A, Inc M, Abbagari S, Houwe A. Exact soliton solutions to the Cahn-Allen equation and Predator-Prey model with truncated M-fractional derivative. *Results Phys* (2022) 37:105455. doi:10.1016/j.rinp.2022.105455

41. Khalil R, Al Horani M, Yousef A, Sababheh M. A new definition of fractional derivative. *J Comput Appl Math* (2014) 264:65–70. doi:10.1016/j.cam.2014.01.002

42. Atangana A, Baleanu D, Alsaedi A. Analysis of time-fractional hunter-saxton equation: A model of neumatic liquid crystal. *Open Phys* (2016) 14:145–9. doi:10.1515/phys-2016-0010

43. Yusuf A, Inc M, Aliyu AI, Baleanu D. Optical solitons possessing beta derivative of the chen-lee-liu equation in optical fibers. *Front Phys* (2019) 7: 00034. doi:10.3389/fphy.2019.00034

44. Hong BJ, Lu DC. Homotopic approximate solutions for the general perturbed Burgers-BBM equation. *J Inf Comput Sci* (2014) 11(11):4003–11. doi:10.12733/jics20104244

45. Zhao HJ, Xuan BJ. Existence and convergence of solutions for the generalized BBM-Burgers equations with dissipative term. *Nonlinear Anal Theor Methods Appl* (1997) 28(11):1835–49. doi:10.1016/s0362-546x(95)00237-p

46. Chen SL, Hou WG. Explicit exact solutions of generalized B-BBM and B-BBM equations. *Acta Physica Sinica* (2001) 50(10):695–8. doi:10.7498/aps.50.1842

47. Mei M. Large-time behavior of solution for generalized Benjamin-Bona-Mahony-Burgers equations. *Nonlinear Anal Theor Methods Appl* (1998) 33: 699–714. doi:10.1016/s0362-546x(97)00674-3

48. Benjamin TB, Bona JL, Mahony JJ. Model equations for long waves in nonlinear dispersive system. *Philos Trans R Soc Lond Ser A: Math Phys Sci* (1972) 272:47–78. doi:10.1098/rsta.1972.0032

49. Mathanaranjan T. Exact and explicit traveling wave solutions to the generalized Gardner and BBMB equations with dual high-order nonlinear terms. *Partial Differential Equations Appl Math* (2021) 4:100120. doi:10.1016/j.padiff.2021.100120

50. Kumar S, Kumar D. Fractional modelling for BBM-Burger equation by using new homotopy analysis transform method. *J Assoc Arab Universities Basic Appl Sci* (2014) 16:16–20. doi:10.1016/j.jaubas.2013.10.002

51. Alharthi MS, Ali HMS, Habib MA, Miah MM, Aljohani AF, Akbar MA, et al. Assorted soliton wave solutions of time-fractional BBM-Burger and Sharma-Tasso-Olver equations in nonlinear analysis. *J Ocean Eng Sci* (2022). doi:10.1016/j.joes.2022.06.022

52. Hossen MB, Roshid HO, Ali MZ. Dynamical structures of exact soliton solutions to Burgers' equation via the bilinear approach. *Partial Differential Equations Appl Math* (2021) 3:100035. doi:10.1016/j.padiff.2021.100035

53. Li LL, Li DF. Exact solutions and numerical study of time fractional Burgers' equations. *Appl Math Lett* (2020) 100:106011. doi:10.1016/j.aml.2019.106011

54. Fukuda I, Ikeda M. Large time behavior of solutions to the Cauchy problem for the BBM-Burgers equation. *J Differential Equations* (2022) 336:275–314. doi:10.1016/j.jde.2022.07.020

55. Oruç Ö. A new algorithm based on Lucas polynomials for approximate solution of 1D and 2D nonlinear generalized Benjamin-Bona-Mahony-Burgers equation. *Comput Math Appl* (2017) 74:3042–57. doi:10.1016/j.camwa.2017.07.046

56. Li C, Guo QL. On the solutions of the space-time fractional coupled Jaulent-Miodek equation associated with energy-dependent Schrödinger potential. *Appl Math Lett* (2021) 121:107517. doi:10.1016/j.aml.2021.107517

57. Gómez S CA, Salas AH, Frias BA. New periodic and soliton solutions for the Generalized BBM and Burgers-BBM equations. *Appl Math Comput* (2010) 217: 1430–4. doi:10.1016/j.amc.2009.05.068

58. Kurt A, Rezazadeh H, Senol M, Neirameh A, Tasbozan O, Eslami M, et al. Two effective approaches for solving fractional generalized Hirota-Satsuma coupled KdV system arising in interaction of long waves. *J Ocean Eng Sci* (2019) 4:24–32. doi:10.1016/j.joes.2018.12.004

59. Akinyemi1 L, Şenol M, Akpan U, Oluwasegun K. The optical soliton solutions of generalized coupled nonlinear Schrödinger-Korteweg-de Vries equations. *Opt Quan Electron* (2021) 53:394. doi:10.1007/s11082-021-03030-7

60. Li ZB, He JH. Fractional complex transform for fractional differential equations. *Math Comput Appl* (2010) 15:970–3. doi:10.3390/mca15050970